DESIGN AND EVALUATION OF A 3D PRINTED FLEXURE FOR A FAST STEERING MIRROR

Johannes Schlarp, Ernst Csencsics, Shingo Ito, and Georg Schitter
Christian Doppler Laboratory for Precision Engineering for Automated In-Line Metrology,
Automation and Control Institute (ACIN), TU Wien, Vienna, Austria
schlarp@acin.tuwien.ac.at

ABSTRACT

This paper presents the simulation and verification of a metallic and a 3D printed flexure for a fast steering mirror. Easy tuning can be important, because by adapting the stiffness of the flexure and thus the resonance frequency of the the system to the scanning application the energy consumption can be reduced. Since the required resonance frequencies change with the application, a flexible manufacturing process, like 3D printing is required. The experimental results show that the measurements of the aluminium flexure match with the simulation. Due to the printing process major deviations between measurement and simulation are observable for the printed flexure, such that a geometrical variation is performed to analyze the influence of the characteristic dimensions on the stiffness of the flexure. Measurement results show that with the arm width the stiffness can be well tuned. It is shown that the power dissipation can be reduced by a factor of 6.8, if the stiffness is adapted to the scanning application.

1. INTRODUCTION

Fast steering mirrors (FSMs) are used in various technical applications, such as scanning optical systems [1], material processing [2] and tracking of objects [3]. Typically FSMs are electromagnetically [4] or piezoelectrically [5] actuated to achieve either a large scan range or high bandwidth, respectively. Their structure can be divided into a static and a moving part. The two parts are typically connected via a flexure, which stabilizes the mover around the pivot point and restricts motion in the non-actuated degrees of freedom [6]. Tuning the suspension mode to a desired frequency in the design phase can be important for the closed-loop control performance and system efficiency. By matching the frequencies with the drive frequencies of the targeted reference scan trajectory, the energy efficiency can be improved [7]. The suspension mode of the actuator is determined by the inertia of the mover and the stiffness of the system, which depends on the characteristic dimensions of the flexure [6]. Flexures are most commonly made out of metal sheets, which are stamped or laser cut, such that an adaptation requires a significant manufacturing effort [8].

3D printing is already a well-established method for rapid prototyping [9] and is of increased importance for the production of final goods [10]. Due to a simple adaptation of printed parts to specific applications, they are already widely used in e.g. medical applications [11]. The most popular 3D printing technique is fused deposition modelling (FDM), which uses plastic filament as the raw material [12]. The plastic is available with a variety of mechanical properties, which ranges from a very stiff carbon fibre reinforced plastic to a rubbery thermoplastic polyurethane (TPU) [12].

The contribution of this paper is the design and evaluation of a 3D printed flexure. Section 2 describes the setup of the used FSM. In Section 3 the design and simulation results of an aluminium and a TPU flexure are presented. The dynamics of both system configurations are measured, analyzed and compared to the results of the simulation in Section 4. The influence of the characteristic dimensions of the flexure on the stiffness are further analyzed in Section 5. Section 6 concludes the paper.

2. FSM SYSTEM

A hybrid reluctance actuated FSM, with an actuation range of $\pm 3°$, is used as a benchmark system. The main components of this actuators are a ferromagnetic core and mover, coils, suspensions and a magnet, which is used to create a DC biasing flux. Thru the coils this flux can be increased/decreased in the first/second air gap between mover and core, which yields to a torque on the mover (further described in [7]). The actuation principle itself is inherently unstable due to the negative stiffness introduced by the reluctance forces, such that a flexure, with a stiffness k of 47 mNm/deg, is required to stabilize the mover

Pre-Print version of the article: J. Schlarp, E. Csencsics, S. Ito, and G. Schitter, "Design and evaluation of a 3D printed flexure for a fast steering mirror", *Proceedings of the 2018 Summer Topical Meeting, Advancing Precision in Additive Manufacturing*, pp.226–231, 2018.

around the pivot point. Since the actuator has a rotational inertia J of 6717 gmm^2, the resonance frequency f_r can be calculated with

$$f_r = \frac{1}{2\pi}\sqrt{\frac{k}{J}} \quad (1)$$

to 100.7 Hz.

3. SIMULATION

Using finite element analysis (FEA) simulations, structural modes and frequency responses of mechanical structures can be determined up front, such that the flexure design can be easily adapted to the specific application. For the simulations, which are performed in ANSYS Mechanical (Ansys, Canonsburg, USA), the material properties need to be set in advance. The metallic flexure is made from aluminium (AW-1050A), with an elastic modulus of 69 GPa and a Poisson ration of 0.3325, while the printed flexure is made out of TPU (Type: Ninjaflex, Ninjatek, Manheim, USA), which has a stated elastic modulus of 12 MPa and a Poisson ratio of 0.4. Both flexures are used to stabilize the moving part of the hybrid reluctance actuated FSM around the pivot point. For the metallic flexure the resonance frequencies of both scan axes are set to 100 Hz, since the flexure is not designed for a specific scan application, while the printed flexure is designed for two different resonance frequencies for investigation purposes and since the drive frequencies of scan trajectories are typically unequal [13]. To compare the results of the two flexures the resonance frequencies of the printed flexure are set to 100 Hz and 130 Hz. The designs and suspension modes of both flexures, which are calculated using modal analysis, are shown in Fig. 1.

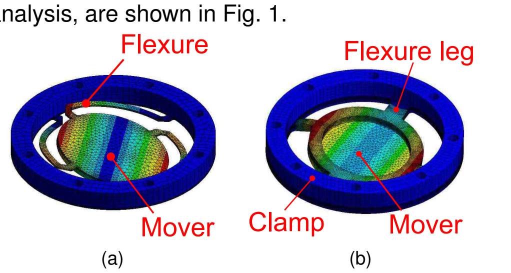

FIGURE 1. Results of the modal analysis. Suspension mode of (a) the aluminium flexure and (b) the 3D printed TPU flexure.

To analyze the system behaviour a harmonic analysis is performed. The results with both flexures are shown in Fig. 2. As can be observed,

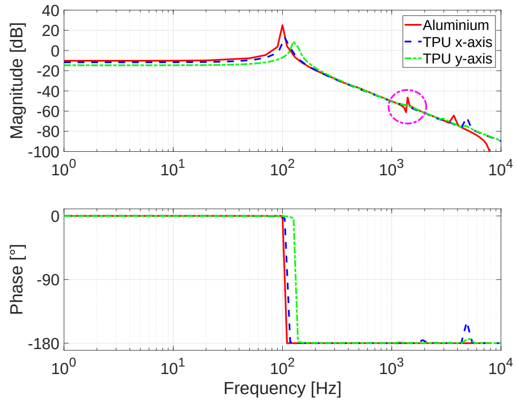

FIGURE 2. Simulated frequency response of the aluminum flexure (red) and the x- (blue) and y-axis (green) of the TPU flexure.

the resonance frequencies match the requirements. Due to the higher damping coefficient of the TPU flexure, the magnitude at the resonance frequency is slightly lower compared to the aluminium flexure. In the frequency response of the aluminium flexure (red solid) a structural mode at 1.4 kHz is observable (magenta circle). For feedback control, such modes be critical, as they can limit the achievable bandwidth [6]. The structural modes of the TPU flexure (blue, green) occur beyond 4 kHz, suggesting that higher control bandwidths may be feasible.

4. EXPERIMENTAL RESULTS

To validate the results of the simulation the system dynamics of both system configurations are measured with a system analyzer (Type: 3562A, Hewlett-Packard, Palo Alto, USA). In Fig. 3 the measured and simulated frequency response of the aluminium flexure is depicted. The measured magnitude response shows good agreement with the simulation in the frequency range of interest up to 1.5 kHz. The frequencies of the suspension mode (100 Hz and 109.6 Hz) and the first structural mode (1.4 kHz and 1.38 kHz) are almost equal for both system axes. In the phase response some deviations are notable, such as the additional phase lag in the measurement caused by the sensor dynamics, sampling delay and eddy currents of the actuator [4]. The measured phase strongly differs above 1.5 kHz, due to the system noise.

The TPU flexure is printed on a 3D printer (Type: Prusa i3 MK3, Prusa, Prague, Czech Republic), which uses the fused deposition modelling method. In Fig. 4 the measurement results of the TPU flexure are compared to the simulation results.

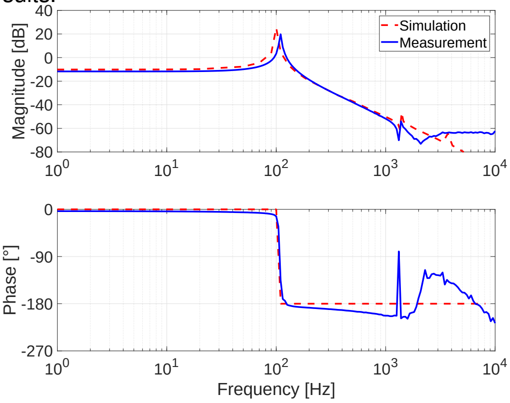

FIGURE 3. Measured and simulated frequency response of the system with the aluminium flexure.

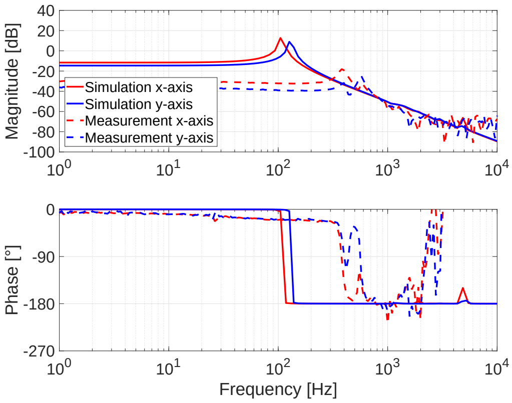

FIGURE 4. Measured and simulated frequency response of the system with the printed TPU flexure.

There are significant deviations observable, which are most likely caused by a change of the mechanical properties of the material during the printing process. The resonance frequencies of the two axes are at 380 Hz and 575 Hz, such that a deviation by a factor of 3.8 - 4 from the designed value can be calculate. Due to the noise floor the measurement is only valid until about 1.5 kHz, such that the structural modes are not observable. The mechanical properties of the material after printing could be determined with a mechanical test bench, such that an accurate simulation model can be generated. However, the elastic modulus and the Poisson ratio strongly depend on various parameters, like the used printer, the printing temperature, the orientation of the part on the printer, etc. [14], such that determined parameter would only be valid for this specific flexure. In order to be able to apply the gained insights to a larger number of 3D printed flexures, the influence of the characteristic dimensions of the flexure on the stiffness are further analyzed.

5. GEOMETRICAL VARIATION

The characteristic dimensions of the printed flexure are the thickness t, the arm widths w_1 and w_2, and the arm length l, which are depicted in Fig. 5.

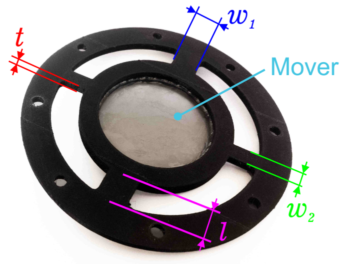

FIGURE 5. Characteristic dimensions of the printed TPU flexure.

The influence of the arm length l can only be analyzed properly, if the outer clamping dimension is also changed. However, due to the mechanical setup of the used FSM, extensive changes would be necessary to manipulate this parameter, such that the arm length is kept constant at 11 mm.

In Fig. 6 the measurement results of printed flexures of various thickness (2 mm - 4 mm) are shown. As can be observed, the frequency of the suspension mode is hardly affected by the flexure thickness (between 340 Hz and 380 Hz). The resonance frequency of the 2 mm flexure is, due to a slight pretension, even higher than the one of the 3 mm flexure. The reason for the low influence of the thickness on the stiffness of the flexure is most likely the high flexibility of the material and the large ratio between arm length (11 mm) and deflection (0.2 mm).

The measurement results for different arm width's are depicted in Fig. 7. As can be observed, by bisecting the width the frequency of the suspension mode is shifted for the tip axis from 367 Hz to 320 Hz and for the tilt axis from 582 Hz to 500 Hz. The resonance frequencies (black dots) are determined out of the measured frequency responses by considering the phase delay of the

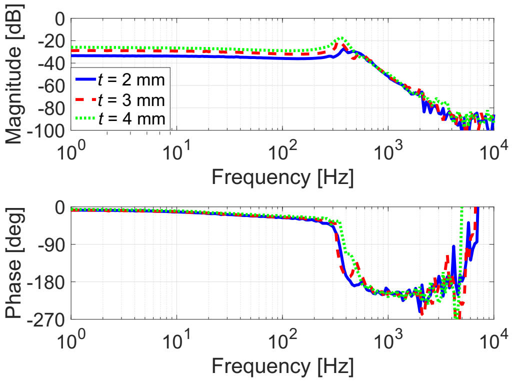

FIGURE 6. Measured frequency response for various TPU flexure thickness.

system, which can be divided into a constant phase shift of 5.5°, a time delay of 500 μs, and the phase shift due to the mechanical resonance of 90°. The resulting reductions of the resonance frequencies are almost equal (12.8 % and 14 %), showing that with the arm width the stiffness of the flexure can be well tuned.

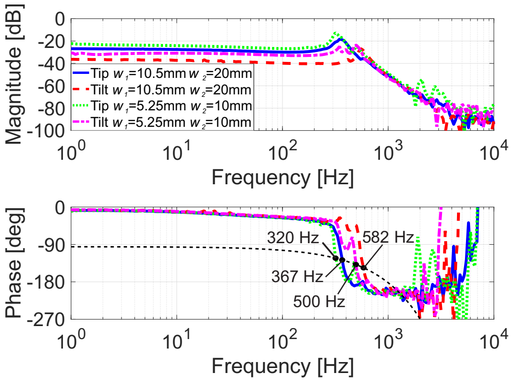

FIGURE 7. Measured frequency response for different flexure arm widths.

To analyze the improvement of the energy efficiency, due to the tuned resonance frequencies, the power dissipation of the actuator is measured at a constant scan amplitude of 0.2° for different flexures. The power dissipation is determined with the measured terminal voltage of the amplifier and the current through the coils (see [4]). Initially the flexure with the following dimensions w_1=10.5 mm and w_2=20 mm is used. At a driving frequency of the sinusoidal signal of 320 Hz for the tip axis, a power dissipation of 27.3 W is measured. The applied frequency matches the resonance frequency of the tip axis of the flexure with the bisected arm width (see Fig. 7). If the same driving signal is applied to the tip axis of this flexure (w_1=5.25 mm and w_2=10 mm), the power dissipation decreases to 4 W. By matching the resonance frequency with the driving frequency, the power consumption can be reduced by a factor of 6.8 for the shown case.

In summary a 3D printed flexure with different resonance frequencies is designed and the influence of the characteristic dimensions on the resonance frequency is shown, revealing that the resonance frequency can be adapted to the scan application and the power consumption can be reduced by a factor of 6.8 by matching the driving frequency with the resonance frequency.

6. CONCLUSION AND FUTURE WORK

In this work a metallic and a 3D printed flexure for a FSM are designed and tested. The results of an FEM simulation are compared to the measured dynamics. The measurement results of the aluminium flexure show good agreement with the simulation, verifying the design. For the printed flexure significant deviations between simulated and measured stiffness are observable, caused by the deviation of the mechanical properties, due to the printing process. Further analysis of the influence of the characteristic dimensions on the stiffness of the flexure shows that the stiffness can be well tuned by adjusting the arm width of the flexure. Tuning the systems resonance frequency to the desired drive frequency, the power dissipation can be reduced by a factor of 6.8. Future work includes the determination of the printed material properties to enable a better prediction of the stiffness and mechanical properties of 3D printed flexures.

ACKNOWLEDGMENTS

The financial support by the Austrian Federal Ministry for Digital and Economic Affairs and the National Foundation for Research, Technology and Development, as well as MICRO-EPSILON MESSTECHNIK GmbH & Co. KG and ATENSOR Engineering and Technology Systems GmbH is gratefully acknowledged.

REFERENCES

[1] Schlarp J, Csencsics E, Schitter G. Optical scanning of laser line sensors for 3D imaging. Applied Optics. 2018;57(18):5242–5248.

[2] Hedding LR. Fast steering mirror design and performance for stabilization and single axis scanning. In: Acquisition, Tracking, and Pointing IV. vol. 1304. International Society for Optics and Photonics; 1990. p. 14.

[3] Mokbel HF, Yuan W, Ying LQ, Hua CG, Roshdy AA. Research on the Mechanical Design of Two-Axis Fast Steering Mirror for Optical Beam Guidance. Proceedings of 2012 International Conference on Mechanical Engineering and Material Science (MEMS 2012). 2012;.

[4] Csencsics E, Schlarp J, Schitter G. High performance hybrid-reluctance-force-based tip/tilt system: Design, control and evaluation. IEEE Transactions on Mechatronics. 2018;Accepted.

[5] Park JH, Lee HS, Lee JH, Yun SN, Ham YB, Yun DW. Design of a piezoelectric-driven tilt mirror for a fast laser scanner. Japanese Journal of Applied Physics. 2012;51(9S2):09MD14.

[6] Munnig Schmidt R, Schitter G, Rankers A, van Eijk J. The Design of High Performance Mechatronics. 2nd ed. Delft: IOS Press; 2014.

[7] Csencsics E, Schitter G. System Design and Control of a Resonant Fast Steering Mirror for Lissajous-based Scanning. IEEE Transactions on Mechatronics. 2017;22(5):1963–1972.

[8] Lobontiu N. Compliant mechanisms: design of flexure hinges. CRC press; 2002.

[9] Mellor S, Hao L, Zhang D. Additive manufacturing: A framework for implementation. International Journal of Production Economics. 2014;149:194–201.

[10] Effenberger I. Multisensorische Inspektion von additiv gefertigten Kunststoffbauteilen. Multisensorik in der Fertigungsmesstechnik 2018. 2018;p. 169–172.

[11] Gibson I, Rosen D, Stucker B. Additive Manufacturing Technologies. New York: Springer; 2014.

[12] Ning F, Cong W, Qiu J, Wei J, Wang S. Additive manufacturing of carbon fiber reinforced thermoplastic composites using fused deposition modeling. Composites Part B: Engineering. 2015;80:369–378.

[13] Tuma T, Lygeros J, Kartik V, Sebastian A, Pantazi A. High-speed multiresolution scanning probe microscopy based on Lissajous scan trajectories. Nanotechnology. 2012;23(18):185501.

[14] Tymrak B, Kreiger M, Pearce JM. Mechanical properties of components fabricated with open-source 3-D printers under realistic environmental conditions. Materials & Design. 2014;58:242–246.